

# HGP-Mamba: Integrating Histology and Generated Protein Features for Mamba-based Multimodal Survival Risk Prediction

Jing Dai<sup>1,2</sup>, Chen Wu<sup>1,2</sup>, Ming Wu<sup>1,2</sup>, Qibin Zhang<sup>1,2</sup>, Zexi Wu<sup>2</sup>,  
Jingdong Zhang<sup>1,2</sup><sup>✉</sup>, and Hongming Xu<sup>1,2,3</sup><sup>✉</sup>

<sup>1</sup> Cancer Hospital of Dalian University of Technology, Shenyang, China  
{jdzhang}@cancerhosp-ln-cmu.com

<sup>2</sup> School of Biomedical Engineering, Faculty of Medicine,  
Dalian University of Technology, Dalian, China

<sup>3</sup> Key Laboratory of Integrated Circuit and Biomedical Electronic System,  
Dalian University of Technology, Dalian, China  
{xmu}@dlut.edu.cn

**Abstract.** Recent advances in multimodal learning have significantly improved cancer survival risk prediction. However, the joint prognostic potential of protein markers and histopathology images remains under-explored, largely due to the high cost and limited availability of protein expression profiling. To address this challenge, we propose HGP-Mamba, a Mamba-based multimodal framework that efficiently integrates histological with generated protein features for survival risk prediction. Specifically, we introduce a protein feature extractor (PFE) that leverages pretrained foundation models to derive high-throughput protein embeddings directly from Whole Slide Images (WSIs), enabling data-efficient incorporation of molecular information. Together with histology embeddings that capture morphological patterns, we further introduce the Local Interaction-aware Mamba (LiAM) for fine-grained feature interaction and the Global Interaction-enhanced Mamba (GiEM) to promote holistic modality fusion at the slide level, thus capture complex cross-modal dependencies. Experiments on four public cancer datasets demonstrate that HGP-Mamba achieves state-of-the-art performance while maintaining superior computational efficiency compared with existing methods. Our source code is publicly available at <https://github.com/Daijing-ai/HGP-Mamba.git>.

**Keywords:** Multimodal learning · Computational Pathology · Multiple Instance Learning · State Space Models · Survival Prediction.

## 1 Introduction

Survival risk prediction is a fundamental task in clinical oncology, aiming to estimate the time to critical events such as death or recurrence and to quantify

---

<sup>✉</sup> Corresponding author

individual mortality risk. Accurate prediction provides essential insights into disease progression, treatment response, and patient prognosis, ultimately guiding personalized therapeutic decision-making [1].

With the rapid advancement of digital pathology, whole slide images (WSIs), as the gold standard, have been increasingly used in survival risk prediction. WSIs provide a comprehensive view of morphological changes at the cellular and tissue levels, offering a critical basis for survival assessment. Given the large number of patches in WSIs, many methods adopt MIL-based methods for efficient processing and analysis, including attention-based MIL models [2,3,4] aim to capture global WSI representations. More recently, transformer-based [5,6] and Mamba-based [7,8,9] architectures leveraging self-attention mechanisms and State Space Models [10] have been introduced, both of which aim to explore mutual-correlations between instances and model long sequence. However, using pathology images alone cannot comprehensively reflect the entire process of cancer occurrence and development. Therefore, the development of robust multimodal approaches is essential yet challenging for constructing accurate and generalizable survival analysis models [11]. With advances in molecular pathology, joint modeling of multimodal data of histology and molecular markers has markedly improved the efficiency and accuracy of survival analysis [12,13]. Previous studies on multi-modal fusion largely focused on pairing histopathology images with genomic data, using techniques like cross-attention [14,15] or optimal transport [16].

Although much progress has been achieved, protein markers, which play a critical role in survival risk prediction, have not been fully explored. This is mainly due to the time-consuming and costly assessment of protein markers, which limits their integration into routine clinical workflows [17]. Protein markers serve as direct functional mediators of cellular processes and provide unique insights into the tumor microenvironment and molecular signaling pathways, thereby complementing the morphological perspective offered by histology images. Recent studies [18,19] has shown the potential of integrating protein marker prediction into histopathology-based prognostic modeling. Nevertheless, they are limited to representative markers, restricting their ability to provide comprehensive biological insights. Moreover, existing frameworks typically focus on specific cancer types, and their broader utility across other cancer types remains to be verified. Furthermore, large-scale WSIs and high-dimensional proteomics profiles pose significant challenges for efficient fine-grained interaction. The quadratic computational complexity of cross-attention mechanisms often lead to the loss of critical patch-level information and increase the risk of overfitting to task-irrelevant features [20], which limits its performance and efficiency, making it difficult in clinical settings.

To address the above challenges, we propose HGP-Mamba, a Mamba-based framework that captures histology and generated protein features while enabling efficient integration of both modalities. Our model directly derives embeddings for up to 50 protein biomarkers simultaneously from WSIs, enabling reliable multimodal survival modeling even in the absence of measured protein pro-

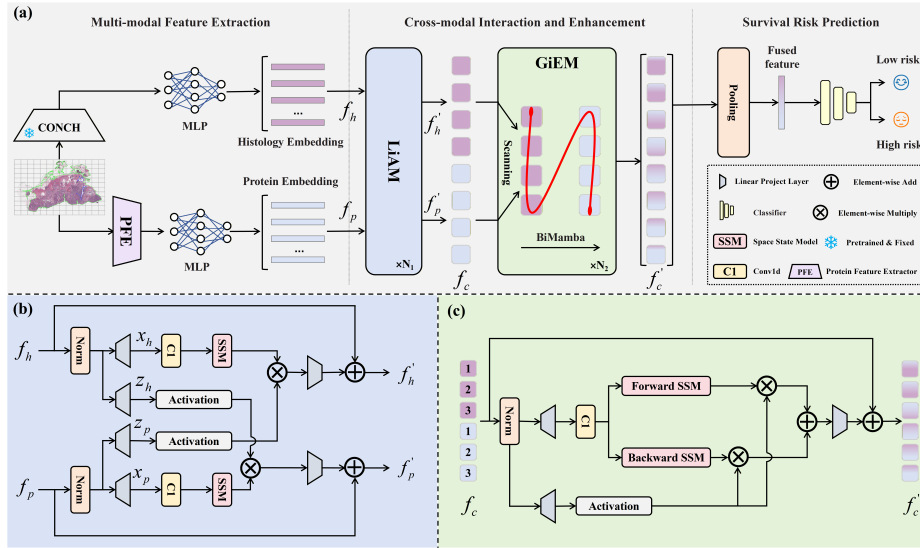


**Fig. 1.** HGP-Mamba overview. (a) Details of the proposed HGP-Mamba which is consisted of three steps: multi-modal feature extraction, feature interaction and enhancement and risk prediction. (b) Schematic of the Local Interaction-aware Mamba (LiAM). (c) Architecture of the Global Interaction-enhanced Mamba (GiEM).

files. Furthermore, we introduce a dual-stage Mamba-based fusion mechanism that achieves local cross-modal interaction and global modality cohesion without the substantial computational overhead typically associated with cross attention architectures. HGP-Mamba bridges the gap between tissue morphology and molecular characteristics, providing a cost-effective and scalable alternative to conventional multimodal prognostic frameworks. Our main contributions are summarized as follows:

- To address the challenges of protein representation learning, we develop a protein feature extractor (PFE) that derives high-throughput protein features directly from WSIs using pretrained foundation models, thereby mitigating data scarcity caused by costly clinical assays.
- We introduce a hierarchical fusion strategy that comprises a Local Interaction-aware Mamba (LiAM) to capture fine-grained inter-modal dependencies and a Global Interaction-enhanced Mamba (GiEM) to ensure holistic modality integration across the entire tissue landscape.
- Extensive experiments across four cancer data cohorts demonstrate the superiority and efficiency of the proposed method compared to state-of-the-art baselines in survival risk prediction.

## 2 Method

The overall architecture of the proposed HGP-Mamba is shown in Fig. 1, which consists of three main stages: multi-modal feature extraction, cross-modal interaction and enhancement, and survival risk prediction. As depicted in Fig. 1(a), each WSI is divided into thousands of non-overlapping patches. Histology and protein embeddings are then independently extracted using two pretrained foundation models. Subsequently, a Local Interaction-aware Mamba (LiAM) along with a Global Interaction-enhanced Mamba (GiEM) are employed to effectively integrate and enhance histology and protein representations. Finally, the fused multimodal features are used to perform survival risk prediction. In the following sections, we first introduce the preliminary knowledge of state space models (SSMs), and then describe the core components of the proposed HGP-Mamba framework.

### 2.1 Space State Models (SSMs)

SSMs can be viewed as linear time-invariant systems that represent a class of sequence models mapping a one-dimensional input signal  $x(t) \in \mathbb{R}$  to an output response  $y(t) \in \mathbb{R}$  via a latent state  $h(t) \in \mathbb{R}^N$ . The system dynamics are formally expressed as:

$$h'(t) = \mathbf{A}h(t) + \mathbf{B}x(t), \quad y(t) = \mathbf{C}h(t), \quad (1)$$

where  $\mathbf{A} \in \mathbb{R}^{N \times N}$  denotes the state transition matrix, and  $\mathbf{B} \in \mathbb{R}^{N \times 1}$  and  $\mathbf{C} \in \mathbb{R}^{N \times 1}$  denote projection matrices.  $h'(t) \in \mathbb{R}^N$  is the derivative of the hidden state.

For practical implementation, SSMs introduce a discretization timescale parameter  $\Delta$  to transform the continuous-time parameters  $\mathbf{A}$ ,  $\mathbf{B}$  into their discrete-time counterparts  $\bar{\mathbf{A}}$ ,  $\bar{\mathbf{B}}$ . The discretization is computed using the Zero-Order Hold (ZOH) method within a specialized CUDA kernel:

$$\bar{\mathbf{A}} = \exp(\Delta\mathbf{A}), \quad \bar{\mathbf{B}} = (\Delta\mathbf{A})^{-1}(\exp(\Delta\mathbf{A}) - I) \cdot \Delta\mathbf{B} \quad (2)$$

After discretization, the SSM can be written in the discrete-time form:

$$h_t = \bar{\mathbf{A}}h_{t-1} + \bar{\mathbf{B}}x_t, \quad y_t = \mathbf{C}h_t \quad (3)$$

Alternatively, the SSM output can be computed using a convolutional formulation, enabling efficient and parallelizable training:

$$\mathbf{K} = (\mathbf{C}\bar{\mathbf{B}}, \mathbf{C}\bar{\mathbf{A}}\bar{\mathbf{B}}, \dots, \mathbf{C}\bar{\mathbf{A}}^{L-1}\bar{\mathbf{B}}), \quad y = \mathbf{x} * \mathbf{K}, \quad (4)$$

where  $*$  denotes the convolution operation,  $\mathbf{K} \in \mathbb{R}^L$  is an SSM kernel, and  $L$  represents the length of the input sequence  $\mathbf{x} = [x(0), \dots, x(L)]$ .

Mamba [7] further extends SSMs by incorporating selection mechanisms, allowing the model parameters to dynamically depend on the input while leveraging an efficient, hardware-aware parallel algorithm. Consequently, Mamba enables effective and efficient long-sequence modeling by selectively propagating or discarding information along the sequence based on the current token [8].

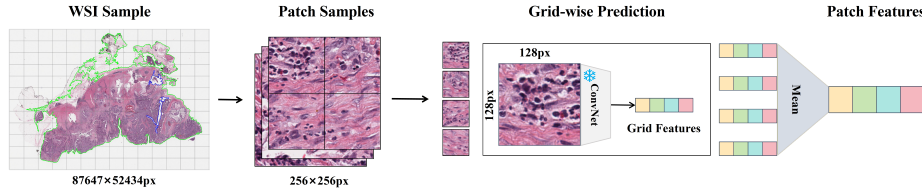


**Fig. 2.** Illustration of our protein feature extractor (PFE). Note that ConvNet is the backbone of the ROISE model.

## 2.2 Multi-modal Feature Extraction

**Histology features** WSIs provide rich morphological information about the tumor microenvironment. However, due to their extremely large size, WSIs cannot be directly processed by convolutional neural networks and need first be partitioned. We begin by segmenting tissue regions, then cut them into  $256 \times 256$  non-overlapping patches at  $20\times$  magnification. We employ a pretrained CONCH model [21], which was initially trained on large-scale WSI-Text pairs, to extract a 512-dimensional embedding for each patch. All patch embeddings from the same WSI are collected as an embedding set. To reduce feature redundancy and computational overhead, we employ a Multi-Layer Perceptron (MLP) to reduce feature dimension and eventually get the histology embedding  $f_h \in \mathbb{R}^{N \times D}$ , where  $N$  denotes the number of patches and  $D = 256$  is the feature dimension.

**Protein features** Protein profiles offer valuable insights into molecular biomarkers associated with cancer prognosis. Given the high cost and limited availability of multiplex protein assays, we leverage ROISE [22], a pretrained foundation model trained on the largest dataset of co-stained H&E and immunostained slides. Unlike prior protein prediction frameworks [18,19], ROISE can simultaneously infer co-expression patterns across up to 50 distinct proteins. Building upon this capability, we develop a Protein Feature Extractor (PFE) to directly derive protein features from WSIs, as illustrated in Fig. 2. Specifically, each WSI patch is partitioned into non-overlapping grids of size  $128 \times 128$ . A ConvNet [23] backbone is then applied to predict expression levels for 50 proteins within each grid. For each marker channel, we compute the mean predicted intensity across all grids, resulting in a normalized  $1 \times M$  feature vector that summarizes the average expression profile at the patch level [24]. Finally, a Multi-Layer Perceptron (MLP) projects this representation to a 256-dimensional protein embedding  $f_p \in \mathbb{R}^{N \times D}$ .

## 2.3 Local Interaction-aware Mamba (LiAM)

To enable fine-grained cross-modal interaction while maintaining computational efficiency, we introduce a novel LiAM module, illustrated in Fig. 1(b). Given

histology and protein features  $f_h$  and  $f_p$ , we first obtain their projected representations  $x_h$  and  $x_p$  by applying layer normalization followed by a linear projection. In parallel,  $f_h$  and  $f_p$  are also projected to  $z_h$  and  $z_p$ , respectively. The specific formulas are as follows:

$$x_m = (\text{Linear}_m^x(\text{Norm}_m(f_m))), \quad m \in \{h, p\} \quad (5)$$

$$z_m = (\text{Linear}_m^z(\text{Norm}_m(f_m))), \quad m \in \{h, p\} \quad (6)$$

Next, intermediate features  $y_h$  and  $y_p$  are computed via a 1D convolution, followed by the SiLU activation and a state space model (SSM):

$$y_m = \text{SSM}(\text{SiLU}(\text{Conv}_{1d}(x_m))), \quad m \in \{h, p\} \quad (7)$$

To refine cross-modal representations,  $y_h$  and  $y_p$  are gated by  $z_p$  and  $z_h$ , respectively, yielding updated outputs  $f'_h$  and  $f'_p$ :

$$f'_h = y_h \odot \text{SiLU}(z_p), \quad f'_p = y_p \odot \text{SiLU}(z_h) \quad (8)$$

Finally, residual connections are incorporated into each modality to facilitate gradient flow, thereby improving stability and convergence. Through this interactive learning mechanism, LiAM effectively captures complementary information and models local cross-modal dependencies.

## 2.4 Global Interaction-enhanced Mamba (GiEM)

Following local cross-modal interaction, we introduce the GiEM module, which employs a bidirectional Mamba (BiMamba) [25] backbone to further strengthen multimodal representations, as illustrated in Fig. 1(c). Unlike Transformer-based approaches that rely on self-attention to process all tokens simultaneously, GiEM adopts an ordered scanning strategy that preserves the sequential nature of Mamba while enabling efficient global interaction modeling. Specifically, given the multimodal feature sequences, we construct a unified representation  $f_c \in \mathbb{R}^{2N \times D}$  by sequentially scanning histology features followed by protein features. This ordered arrangement ensures that information from both modalities is processed in a structured manner, allowing Mamba’s selective scanning mechanism to effectively capture both intra- and inter-modal dependencies.

## 2.5 Survival Risk Prediction

The GiEM module outputs a processed feature sequence  $f'_c \in \mathbb{R}^{2N \times D}$ , which is then aggregated via max pooling to yield a global feature vector. This vector is subsequently passed into a linear classifier to generate the final survival risk prediction. Following prior studies [14,15], we simplify the original event time regression problem to a classification problem by dividing the continuous timeline into  $n$  intervals. The interval  $t_k$  in which the event occurs is used as the class label  $k$ . The model predicts a hazard vector  $H = \{h_1, \dots, h_k, \dots, h_n\}$ , where  $h_k$

**Table 1.** C-index( $\uparrow$ ) performance(mean  $\pm$  std) over four datasets. The best and second best results are highlighted in red and blue, respectively.

Model	Datasets				Overall
	COADREAD	KIRC	KIRP	LIHC	
Mean-Pooling	0.673 $\pm$ 0.055	0.729 $\pm$ 0.048	0.818 $\pm$ 0.065	0.708 $\pm$ 0.059	0.732
Max-Pooling	0.603 $\pm$ 0.056	0.715 $\pm$ 0.053	0.782 $\pm$ 0.069	0.657 $\pm$ 0.094	0.689
ABMIL [2]	0.689 $\pm$ 0.071	0.741 $\pm$ 0.045	0.791 $\pm$ 0.099	0.721 $\pm$ 0.075	0.736
CLAM-SB [4]	0.681 $\pm$ 0.041	0.736 $\pm$ 0.055	<b>0.838<math>\pm</math>0.046</b>	0.714 $\pm$ 0.083	<b>0.742</b>
CLAM-MB [4]	0.644 $\pm$ 0.069	0.744 $\pm$ 0.036	0.812 $\pm$ 0.075	0.702 $\pm$ 0.070	0.726
TransMIL [6]	<b>0.695<math>\pm</math>0.034</b>	0.714 $\pm$ 0.051	0.797 $\pm$ 0.063	0.717 $\pm$ 0.078	0.731
MambaMIL [8]	0.674 $\pm$ 0.082	0.728 $\pm$ 0.065	0.815 $\pm$ 0.034	<b>0.732<math>\pm</math>0.060</b>	0.737
BiMambaMIL [8]	0.683 $\pm$ 0.087	0.739 $\pm$ 0.039	0.796 $\pm$ 0.045	0.729 $\pm$ 0.071	0.737
SRMambaMIL [8]	0.676 $\pm$ 0.085	<b>0.751<math>\pm</math>0.029</b>	0.793 $\pm$ 0.040	0.732 $\pm$ 0.068	0.738
HGP-Mamba (Ours)	<b>0.695<math>\pm</math>0.069</b>	<b>0.755<math>\pm</math>0.035</b>	<b>0.842<math>\pm</math>0.054</b>	<b>0.739<math>\pm</math>0.079</b>	<b>0.758</b>

denotes the conditional probability of the event occurring in the  $k$ -th interval. Each sample is represented as  $\{H, c, k\}$ , where  $c \in \{0, 1\}$  indicates the censoring status. The discrete survival function is defined as  $f_{\text{surv}}(H, k) = \prod_{i=1}^k (1 - h_i)$ . The survival risk prediction loss is formulated as:

$$\begin{aligned}
 L_{\text{surv}} = & -c \log(f_{\text{sur}}(H, k)) \\
 & - (1 - c) \log(f_{\text{sur}}(H, k - 1)) \\
 & - (1 - c) \log(h_k).
 \end{aligned} \tag{9}$$

## 3 Experiments

### 3.1 Datasets and Metrics

We conducted experiments on four cancer cohorts derived from The Cancer Genome Atlas (TCGA)<sup>4</sup>, including Colon and Rectum Adenocarcinoma (COAD-READ,  $n = 551$ ), Kidney Clear Cell Carcinoma (KIRC,  $n = 498$ ), Kidney Papillary Cell Carcinoma (KIRP,  $n = 261$ ), Liver Cancer (LIHC,  $n = 311$ ), and Lung Adenocarcinoma (LUAD,  $n = 455$ ). For cases with multiple slides, one was randomly selected for analysis. We trained the models to predict overall survival (OS) risk and assessed performance using the cross-validated concordance index (C-index) [26], which evaluates how well a survival model ranks patients with their survival time compared to actual survival outcomes.

### 3.2 Implementation Details

We employed 5-fold cross-validation to evaluate our model and other compared methods. We set the number of LiAM blocks  $N_1 = 2$  and the number of GiEM

<sup>4</sup> <https://portal.gdc.cancer.gov/>

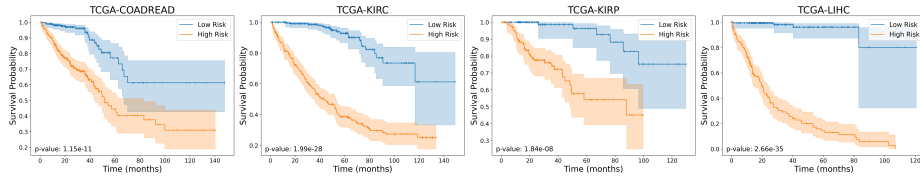


**Fig. 3.** Kaplan-Meier survival curves of the proposed model on four cancer datasets.

blocks  $N_2 = 1$ . Training was conducted for up to 100 epochs with early stopping based on validation C-index. Each epoch used a batch size of 1, with gradients accumulated over 32 steps before backpropagation. The Adam optimizer was used with a learning rate of  $2e-4$  and a weight decay of  $1e-5$ . During training, a weighted sampling strategy was employed to mitigate class imbalance across all tasks. All experiments were conducted using PyTorch running on a single NVIDIA RTX 4090 GPU.

### 3.3 Comparison Results

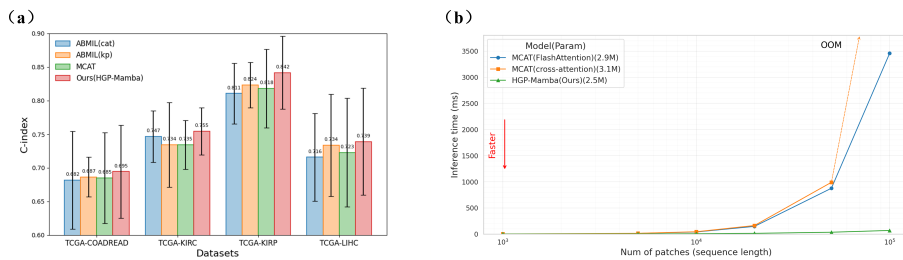
To demonstrate the effectiveness of HGP-Mamba, we compare it with following methods: **(1)** conventional pooling methods, including Mean Pooling and Max Pooling; **(2)** attention-based methods, including ABMIL [2], CLAM [4] with its two variants CLAM-SB and CLAM-MB; **(3)** Transformer-based TransMIL [6]; **(4)** Mamba-based methods [8], including MambaMIL, BiMambaMIL, and SR-MambaMIL. Table 1 presents the comparative results, where our proposed HGP-Mamba achieves an average C-index of 75.8%, surpassing all other comparative methods. Specifically, HGP-Mamba outperforms all prior approaches on the KIRC, KIRP and LIHC datasets and ties for first place with TransMIL on the COADREAD dataset. These results underscore the efficacy of HGP-Mamba in effectively integrating multimodal features and highlight the advantages of multimodal learning for survival prediction.

### 3.4 Patient Stratification

To further validate the effectiveness of HGP-Mamba for survival analysis, we divided all patients into low-risk and high-risk groups according to the median predicted risk scores generated by HGP-Mamba. Kaplan-Meier (KM) analysis was then performed to visualize the survival outcomes across the two groups, as illustrated in Fig. 3. Statistical significance between the risk groups was assessed using the Log-rank test, with a p-value less than 0.05 considered significant. As shown in Fig. 3, all datasets yielded p-values well below 0.05, demonstrating the strong discriminatory ability of HGP-Mamba in survival risk prediction.

**Table 2.** Ablation study assessing the impact of three key modules in HGP-Mamba.

Configuration	Datasets			
	COADREAD	KIRC	KIRP	LIHC
w/o PFE	0.687 ± 0.064	0.739 ± 0.027	0.786 ± 0.119	0.715 ± 0.087
w/o LiAM	0.629 ± 0.067	0.751 ± 0.045	0.781 ± 0.109	0.711 ± 0.083
w/o GiEM	0.681 ± 0.071	0.744 ± 0.045	0.800 ± 0.082	0.727 ± 0.079
Full (HGP-Mamba)	<b>0.695 ± 0.069</b>	<b>0.755 ± 0.035</b>	<b>0.842 ± 0.054</b>	<b>0.739 ± 0.079</b>

**Fig. 4.** (a) Comparison of different multimodal fusion methods. (b) Inference time comparison with varying patches

### 3.5 Ablation Studies

**Effectiveness of proposed components** We performed ablation studies in Table 2 to evaluate the contributions of the proposed components. First, removing the PFE module reduces HGP-Mamba into a MIL method similar to BiMambaMIL, leading to a significant drop in C-index (e.g., from 0.842 to 0.786 on KIRP). This highlights that the PFE provides prognostic information complementary to raw histological representations.

Next, excluding the LiAM module significantly diminishes the model’s capacity to model fine-grained inter-modal interactions, resulting in a notable decline in C-index. LiAM utilizes a gating mechanism that dynamically weighs the interaction between histology and protein features, which can learn to suppress noisy influence during the training process. This design ensures robust survival risk prediction.

Finally, omitting the GiEM module degraded modality cohesion and produced suboptimal performance. Overall, these ablations confirm that PFE, LiAM, and GiEM each play essential and complementary roles. Together, they provide a comprehensive representation of tumor morphology and molecular heterogeneity, which is essential for accurate survival risk prediction.

**Superiority of multimodal fusion method** To further demonstrate the superiority of our multimodal interaction and enhancement modules, we replaced

LiAM and GiEM with several baseline fusion method for survival risk prediction. First, we incorporated two common late-fusion schemes using ABMIL with feature concatenation (ABMIL-Cat) [27], and ABMIL with a Kronecker Product fusion (ABMIL-KP) [28]. As shown in Fig. 4(a), both approaches underperform relative to HGP-Mamba, indicating their limited ability to capture complex tumor–microenvironment relationships. We also compared HGP-Mamba with the leading early fusion method, MCAT [14,18,19]. Because of GPU memory constraints, we substituted MCAT’s cross-attention module with FlashAttention [29] in our implementation. Our method leverages the dual-stage Mamba architecture, achieving superior predictive performance while preserving high computational efficiency.

Moreover, we conducted efficiency analysis using parameter count and inference time. For fairness, the comparison focuses exclusively on the cross-modal interaction and enhancement stage and excludes the cost of multimodal feature extraction; all experiments were executed under identical conditions. We benchmarked HGP-Mamba against the Transformer-based MCAT implemented with its two core attention mechanisms (co-attention and FlashAttention). Specifically, we constructed histology embedding sequences of length 1,000, 5,000, 10,000, 20,000, 50,000, and 100,000 with an embedding dimension of 512, while keeping protein embeddings fixed at dimension 50.

As shown in Fig. 4(b), HGP-Mamba has a substantially smaller parameter footprint (2.47 MB) than the Transformer baselines and consistently achieves large speedups across all sequence lengths. For example, when processing 50,000 tokens, HGP-Mamba requires only 34.08 ms, representing a 96.1% and 96.6% reduction in inference time compared with FlashAttention-based MCAT (875.26 ms) and co-attention MCAT (988.73 ms), respectively. These results indicate that HGP-Mamba not only maintains stable predictive performance for survival risk but also offers a major advantage in computational efficiency for cross-modal interaction.

### 3.6 Protein Visualization

To validate whether the PFE captures authentic molecular signals, we visualized protein expression patterns (e.g., PD-L1) across the TCGA-COADREAD cohort. As shown in Figure 5, the predicted high-expression areas (red) exhibit strong spatial concordance with histologically confirmed tumor regions. Detailed ROI analysis further demonstrates that the inferred signals are confined to specific biological compartments, such as tumor nests and stroma with immune infiltration. This consistency with pathological ground truth suggests that HGP-Mamba successfully bridges the gap between raw morphology and underlying molecular heterogeneity.

## 4 Conclusion

In this work, we propose HGP-Mamba, a Mamba-based framework that captures histology and generated protein features while enabling efficient integration of

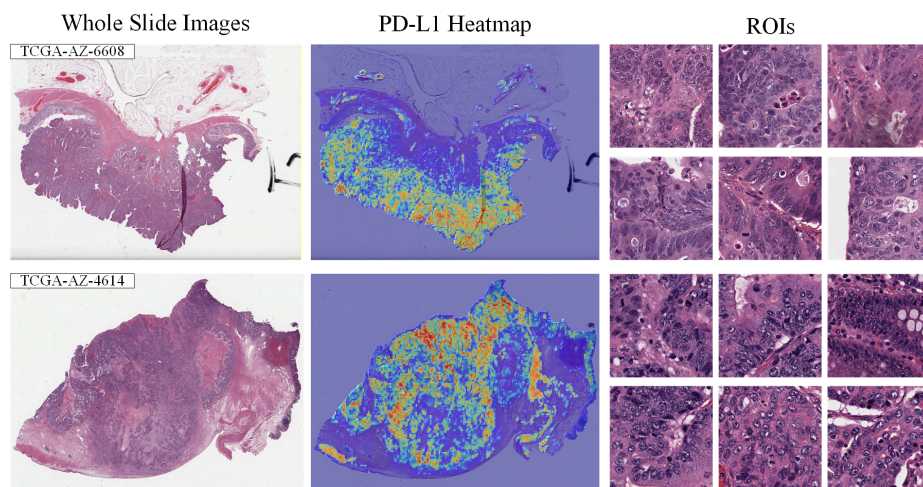


**Fig. 5.** Spatial expression heatmaps for PD-L1 on randomly selected slides from the TCGA-COADREAD dataset. For each sample, the left panel shows the WSI thumbnail, the middle panel overlays the predicted PD-L1 expression heatmap on the WSI, and the right panel displays the selected patches according to the predicted expression level.

both modalities. By leveraging pretrained foundation models, HGP-Mamba directly extracts high-throughput protein features from WSIs, thereby mitigating the scarcity of measured protein profiles. Through Mamba-based cross-modal interaction and enhancement, the framework effectively captures tumor heterogeneity and yields a more comprehensive representation for cancer survival risk prediction. Given its superiority and efficiency, HGP-Mamba can be extended to more complex tasks involving diverse data modalities, facilitating future translation toward clinical applications.

## References

1. Simon Wiegrebe, Philipp Kopper, Raphael Sonabend, Bernd Bischl, and Andreas Bender. Deep learning for survival analysis: a review. *Artificial Intelligence Review*, 57(3):65, 2024.
2. Maximilian Ilse, Jakub Tomczak, and Max Welling. Attention-based deep multiple instance learning. In *International conference on machine learning*, pages 2127–2136. PMLR, 2018.
3. Jiawen Yao, Xinliang Zhu, Jitendra Jonnagaddala, Nicholas Hawkins, and Junzhou Huang. Whole slide images based cancer survival prediction using attention guided deep multiple instance learning networks. *Medical image analysis*, 65:101789, 2020.
4. Ming Y Lu, Drew FK Williamson, Tiffany Y Chen, Richard J Chen, Matteo Barbieri, and Faisal Mahmood. Data-efficient and weakly supervised computational pathology on whole-slide images. *Nature biomedical engineering*, 5(6):555–570, 2021.

5. Shuai Jiang, Arief A Suriawinata, and Saeed Hassanpour. Mhattnsurv: Multi-head attention for survival prediction using whole-slide pathology images. *Computers in biology and medicine*, 158:106883, 2023.
6. Zhuchen Shao, Hao Bian, Yang Chen, Yifeng Wang, Jian Zhang, Xiangyang Ji, et al. Transmil: Transformer based correlated multiple instance learning for whole slide image classification. *Advances in neural information processing systems*, 34:2136–2147, 2021.
7. Albert Gu and Tri Dao. Mamba: Linear-time sequence modeling with selective state spaces. In *First conference on language modeling*, 2024.
8. Shu Yang, Yihui Wang, and Hao Chen. Mambamil: Enhancing long sequence modeling with sequence reordering in computational pathology. In *International conference on medical image computing and computer-assisted intervention*, pages 296–306. Springer, 2024.
9. Haiqin Zhong, Meidan Ding, Cheng Zhao, Yongtao Zhang, Tianfu Wang, and Baiying Lei. Msmmil: Multi-scan mamba-based multiple instance learning for whole slide image classification. *Knowledge-Based Systems*, 324:113871, 2025.
10. Rudolph Emil Kalman. A new approach to linear filtering and prediction problems. 1960.
11. Kevin M Boehm, Pegah Khosravi, Rami Vanguri, Jianjiong Gao, and Sohrab P Shah. Harnessing multimodal data integration to advance precision oncology. *Nature Reviews Cancer*, 22(2):114–126, 2022.
12. Richard J Chen, Ming Y Lu, Jingwen Wang, Drew FK Williamson, Scott J Rodig, Neal I Lindeman, and Faisal Mahmood. Pathomic fusion: an integrated framework for fusing histopathology and genomic features for cancer diagnosis and prognosis. *IEEE Transactions on Medical Imaging*, 41(4):757–770, 2020.
13. Fengtao Zhou and Hao Chen. Cross-modal translation and alignment for survival analysis. In *Proceedings of the IEEE/CVF International Conference on Computer Vision*, pages 21485–21494, 2023.
14. Richard J Chen, Ming Y Lu, Wei-Hung Weng, Tiffany Y Chen, Drew FK Williamson, Trevor Manz, Maha Shady, and Faisal Mahmood. Multimodal co-attention transformer for survival prediction in gigapixel whole slide images. In *Proceedings of the IEEE/CVF international conference on computer vision*, pages 4015–4025, 2021.
15. Guillaume Jaume, Anurag Vaidya, Richard J Chen, Drew FK Williamson, Paul Pu Liang, and Faisal Mahmood. Modeling dense multimodal interactions between biological pathways and histology for survival prediction. In *Proceedings of the IEEE/CVF Conference on Computer Vision and Pattern Recognition*, pages 11579–11590, 2024.
16. Yingxue Xu and Hao Chen. Multimodal optimal transport-based co-attention transformer with global structure consistency for survival prediction. In *Proceedings of the IEEE/CVF international conference on computer vision*, pages 21241–21251, 2023.
17. Sarah Black, Darci Phillips, John W Hickey, Julia Kennedy-Darling, Vishal G Venkatarahaman, Nikolay Samusik, Yury Goltsev, Christian M Schürch, and Garry P Nolan. Codex multiplexed tissue imaging with dna-conjugated antibodies. *Nature protocols*, 16(8):3802–3835, 2021.
18. Sonali Andani, Boqi Chen, Joanna Ficek-Pascual, Simon Heinke, Ruben Casanova, Bernard Friedrich Hild, Bettina Sobottka, Bernd Bodenmiller, Viktor H Koelzer, et al. Histopathology-based protein multiplex generation using deep learning. *Nature Machine Intelligence*, pages 1–16, 2025.

19. Zhe Li, Yuchen Li, Jinxi Xiang, Xiyue Wang, Sen Yang, Xiaoming Zhang, Feiyisope Eweje, Yijiang Chen, Xiangde Luo, Yuanyuan Li, et al. Ai-enabled virtual spatial proteomics from histopathology for interpretable biomarker discovery in lung cancer. *Nature Medicine*, pages 1–14, 2026.
20. Chengsheng Zhang, Linhao Qu, Xiaoyu Liu, and Zhijian Song. Me-mamba: Multi-expert mamba with efficient knowledge capture and fusion for multimodal survival analysis. *arXiv preprint arXiv:2509.16900*, 2025.
21. Ming Y Lu, Bowen Chen, Drew FK Williamson, Richard J Chen, Ivy Liang, Tong Ding, Guillaume Jaume, Igor Odintsov, Long Phi Le, Georg Gerber, et al. A visual-language foundation model for computational pathology. *Nature medicine*, 30(3):863–874, 2024.
22. Eric Wu, Matthew Bieniosek, Zhenqin Wu, Nitya Thakkar, Gregory W Charville, Ahmad Makky, Christian M Schürch, Jeroen R Huyghe, Ulrike Peters, Christopher I Li, et al. Rosie: Ai generation of multiplex immunofluorescence staining from histopathology images. *Nature Communications*, 16(1):7633, 2025.
23. Zhuang Liu, Hanzi Mao, Chao-Yuan Wu, Christoph Feichtenhofer, Trevor Darrell, and Saining Xie. A convnet for the 2020s. In *Proceedings of the IEEE/CVF conference on computer vision and pattern recognition*, pages 11976–11986, 2022.
24. Muhammad Shaban, Yuzhou Chang, Huaying Qiu, Yao Yu Yeo, Andrew H Song, Guillaume Jaume, Yuchen Wang, Luca L Weishaupt, Tong Ding, Anurag Vaidya, et al. A foundation model for spatial proteomics. *arXiv preprint arXiv:2506.03373*, 2025.
25. Lianghai Zhu, Bencheng Liao, Qian Zhang, Xinlong Wang, Wenyu Liu, and Xinggang Wang. Vision mamba: Efficient visual representation learning with bidirectional state space model. *arXiv preprint arXiv:2401.09417*, 2024.
26. Patrick J Heagerty and Yingye Zheng. Survival model predictive accuracy and roc curves. *Biometrics*, 61(1):92–105, 2005.
27. Pooya Mobadersany, Safoora Yousefi, Mohamed Amgad, David A Gutman, Jill S Barnholtz-Sloan, José E Velázquez Vega, Daniel J Brat, and Lee AD Cooper. Predicting cancer outcomes from histology and genomics using convolutional networks. *Proceedings of the National Academy of Sciences*, 115(13):E2970–E2979, 2018.
28. Richard J Chen, Ming Y Lu, Drew FK Williamson, Tiffany Y Chen, Jana Lipkova, Zahra Noor, Muhammad Shaban, Maha Shady, Mane Williams, Bumjin Joo, et al. Pan-cancer integrative histology-genomic analysis via multimodal deep learning. *Cancer cell*, 40(8):865–878, 2022.
29. Tri Dao, Dan Fu, Stefano Ermon, Atri Rudra, and Christopher Ré. Flashattention: Fast and memory-efficient exact attention with io-awareness. *Advances in neural information processing systems*, 35:16344–16359, 2022.